

# Merging of the Dielectric $\alpha$ and $\beta$ Relaxations in Glass-Forming Polymers

D. Gómez, A. Alegria, A. Arbe, and J. Colmenero\*

Departamento de Física de Materiales Universidad del País Vasco, and Unidad de Física de Materiales (CSIC-UPV/EHU), Apdo. 1072, 20080 San Sebastián, Spain

Received December 6, 1999

**ABSTRACT:** The merging of the main and the secondary dielectric relaxations in a series of six polymers has been investigated by using broadband dielectric spectroscopy ( $10^{-2}$ – $10^9$  Hz). The data have been analyzed in two different ways. In one case, the whole relaxation process has been modeled by the simple addition of the relaxation functions corresponding to the main and secondary relaxations. In the other case, we have used the approach first proposed by Williams and Watts (Williams, G.; Watts, C.D. In *NMR, Basic Principles and Progress*; Diehl, P., Fluck, E., Kosfeld R., Eds.; Springer-Verlag, Berlin, 1971; Vol. 4, pp 271–285). This approach can be formally reduced to the addition of two terms, one corresponding to the main relaxation and the other to a combination of the functions corresponding to the main and secondary relaxations extrapolated from low temperatures. Both methods of analysis happen to describe the experimental data successfully in the merging region. In the framework of the Williams and Watts approach, the experimental behavior in the merging range is explained simply as a natural consequence of the extrapolation of the low-temperature relaxation behavior. However, using the simple addition method, this is not possible, which in this framework would be interpreted as due to a change of the secondary relaxation mechanism in the merging region. Therefore, the Williams and Watts approach provides the simplest physical picture for describing the merging of the  $\alpha$  and  $\beta$  relaxations. Finally, the results obtained in this framework are interpreted using a free-energy landscape model.

## I. Introduction

The dynamics of amorphous polymers and other glass-forming systems has been intensively investigated over the past few decades. From a phenomenological point of view, it is well established that the dynamical process responsible for the main relaxation, commonly termed as  $\alpha$  relaxation, is related to the glass-transition process.<sup>1–4</sup> In addition to the  $\alpha$  relaxation, which is universally observed in every glass forming system, another dynamical process, usually referred to as the Johari–Goldstein  $\beta$  process, or secondary relaxation,<sup>5,6</sup> is also observed in most of the glass-forming systems. Contrarily to the  $\alpha$  relaxation, which involves cooperative molecular motions, the  $\beta$  process has been commonly attributed to local rearrangements. Nevertheless, the microscopic origin of both processes is still far from being well understood.<sup>7–9</sup> However, these dynamical processes, when studied in the range where they are well separated, show a series of characteristics which seems to be universal. The spectral shape of both processes is in general very different from that corresponding to a single Debye-like process. Although the shape of the  $\alpha$  process is essentially temperature independent, the relaxation spectra of the  $\beta$  process narrow systematically with increasing temperature. On the other hand, although the characteristic time of the  $\beta$  relaxation shows an Arrhenius-like temperature dependence, the time scale of the  $\alpha$  relaxation is non-Arrhenius and tends to diverge some tens of degrees below the temperature range experimentally accessible (the lowest temperature accessible is a few degrees below the glass transition temperature  $T_g$ ).<sup>10</sup> These very different temperature dependences often lead to the fact that the characteristic times of the two processes become comparable at high temperature/frequency. This range is usually referred to as the “merging region” or the

“splitting region”. In the majority of the systems investigated so far, an extrapolation of the temperature dependences from low temperature to temperatures above the merging region, would imply that, at high temperatures, the more local  $\beta$  process would become slower than the cooperative  $\alpha$  relaxation, a behavior which has never been observed. This feature was pointed out, more than 20 years ago, by Williams and Watts.<sup>11</sup> To explain this apparent paradox, these authors developed a molecular model which assumes that the dynamics of each individual entity is driven by two different molecular mechanisms. The fast molecular motions involved in the  $\beta$  relaxation are attributed to restricted motions in a fixed environment which allow a partial relaxation. Only when the  $\alpha$  relaxation mechanisms are able to break down the environment is the whole relaxation achieved. In the simplest case where only autocorrelation terms are considered, which is a simplification of the general concept given by Williams and Watts, the whole relaxation function in the time domain is given by

$$\varphi(t) = \varphi_\alpha(t)[f_\alpha + (1 - f_\alpha)\varphi_\beta(t)] \quad (1)$$

where  $\varphi_\alpha(t)$  and  $\varphi_\beta(t)$  correspond to the normalized (ranging from 1 down to 0) relaxation functions of the  $\alpha$  and  $\beta$  processes, respectively, and  $1 - f_\alpha$  accounts for the fraction of the relaxation allowed by the mechanisms involved in the  $\beta$  process. This approach will be referred in the following as WW ansatz. As commented above, when both processes are well separated, the  $\varphi_\alpha(t)$  decay is not significant until the  $\beta$  relaxation is complete (i.e.,  $\varphi_\alpha(t) \approx 1$  when  $\varphi_\beta(t) \approx 0$ ) and therefore, eq 1 can be rewritten as

$$\varphi(t) = f_\alpha \varphi_\alpha(t) + (1 - f_\alpha)\varphi_\beta(t) \quad (2)$$

This equation has been extensively used in the literature to analyze data, since for a long time the typical relaxation measurements on polymers (mainly dielectric and mechanical spectroscopies) were performed in the temperature range where the relaxation times of the  $\alpha$  and  $\beta$  processes are very different, i.e., where eqs 1 and 2 are equivalent. Only recently, have high-frequency accurate dielectric measurements on polymeric systems become available, making the range of temperatures where the  $\alpha$  and  $\beta$  processes are very close to each other accessible (merging range).

In a series of very recent works, the WW ansatz has been successfully used for the analysis of the high-temperature dynamics of both, polymers and low molecular mass glass-forming liquids.<sup>12–15</sup> In these studies, it was found that the whole dielectric relaxation at high temperature can be described by means of eq 1 when  $\varphi_\alpha(t)$  and  $\varphi_\beta(t)$  are built by extrapolation from the low temperatures, where both can be determined independently. Furthermore, the analysis of the neutron spin echo data of 1,4 polybutadiene in the same temperature range measured dielectrically seems to support these results.<sup>12</sup>

On the other hand, also recently,<sup>16–19</sup> high-frequency measurements on a series of polymers have been analyzed in terms of eq 2. In this framework, which in the following will be referred to as “addition ansatz”, it is found that the characteristics of  $\varphi_\beta(t)$  change at high temperature, mainly because the characteristic time of the  $\beta$  relaxation does not follow the low-temperature Arrhenius behavior any longer but deviates toward faster times. This behavior has been interpreted by the authors as a proof that there exists a change in the polymer dynamics mechanism in the temperature range where the  $\alpha$  and  $\beta$  relaxations merge. The reason for this conclusion is that some degrees above this temperature region, the difference between the (extrapolated) heat capacity of the glassy polymer and that of the melt seems to extrapolate to zero. This finding has been interpreted by these authors as a signature of missing of cooperativity in the dynamics of polymer melts above this temperature.

From the theoretical point of view, eq 1 is also supported by the results obtained in the framework of a free-energy landscape model for the dynamics of glass-forming systems,<sup>20</sup> when a slow secondary relaxation is considered.<sup>21</sup> In this model the  $\beta$  relaxation is attributed to restricted angular fluctuations, modeled by a superposition of simple two-site angular jumps within a cone of angle  $\theta$ , whereas the  $\alpha$  relaxation occurs via isotropic tumbling of the jump axis. In this framework, it is found that eq 1 allows a rather good description of the relaxation behavior in the merging region in the general case, and it gives the exact solution for the particular case in which the two relaxation mechanisms are totally uncorrelated.

Trying to clarify the general validity of the WW ansatz for the analysis of the relaxation behavior of polymers and the subsequent implications about the polymer melt dynamics at high temperature, in this work we have investigated several polymer systems in a wide temperature range. The polymers selected belong to different families having very different characteristics (glass transition temperatures, fragility, structure, ...) so the conclusions obtained would be valid in general for the dynamics of polymers in the merging region. We have used broad-band dielectric spectroscopy since it combines a very broad frequency range with a high

resolution, which allows to investigate in detail the relaxation processes in a very wide temperature range, of typically more than 200 K.

The paper is organized as follows: In section II a detailed description of the two different ansatzs that will be used in the analysis of the experimental data is presented. Section III gives a short description of the experimental techniques used and the polymers investigated. In section IV, the relaxation behavior of the polymers is investigated and the results of the analysis are depicted. In section V, the descriptions obtained in the framework of the two different ansatzs are compared and the implications of such a comparison are discussed. Finally, the conclusions of this study are summarized in section VI.

## II. Approaches for the Data Analysis

A detailed comparison between the physical grounds of the addition and the WW ansatz can be found elsewhere.<sup>22</sup> The main objective of this section is to summarize how the two different methods of analysis have been applied to the dielectric relaxation data in the present investigation. In a dielectric relaxation experiment, the frequency dependent complex permittivity  $\epsilon^*(\omega)$  can generally be expressed as

$$\epsilon^*(\omega) = (\epsilon_s - \epsilon_\infty)\Phi^*(\omega) + \epsilon_\infty \quad (3)$$

where  $\Phi^*(\omega)$ , which in the following will be referred to as normalized relaxation function, is connected via a Laplace transformation with the time derivative of  $\varphi(t)$ , and  $\epsilon_s$  and  $\epsilon_\infty$  are the static value and the high-frequency limiting value of the permittivity, respectively. When two different processes ( $\alpha$  and  $\beta$  in our case) contribute to the dielectric complex permittivity, the addition ansatz is the simplest empirical approach that one can imagine. In this case, eq 3 can be written in as

$$(\epsilon^*(\omega) - \epsilon_\infty)/(\epsilon_s - \epsilon_\infty) = \Phi^*(\omega) = f_\alpha \Phi_\alpha^*(\omega) + (1 - f_\alpha)\Phi_\beta^*(\omega) \quad (4)$$

where  $\Phi_\alpha^*(\omega)$  and  $\Phi_\beta^*(\omega)$  are now the normalized relaxation functions corresponding to the two processes considered. It is clear that eq 4 implies  $\Delta\epsilon = \Delta\epsilon_\alpha + \Delta\epsilon_\beta$ , where  $\Delta\epsilon = \epsilon_s - \epsilon_\infty$ ,  $\Delta\epsilon_\alpha = \Delta\epsilon f_\alpha$  and  $\Delta\epsilon_\beta = \Delta\epsilon (1 - f_\alpha)$ . The counterpart of eq 4 in the time domain has the form of eq 2.

It is well-known that the relaxation functions  $\Phi_\alpha^*(\omega)$  and  $\Phi_\beta^*(\omega)$  are not simple Debye functions, [i.e.,  $\varphi_\alpha(t)$  and  $\varphi_\beta(t)$  are not simple exponentials]. However, these non-Debye (nonexponential) functions can formally be expressed in terms of empirical distribution functions of Debye (exponential) processes. Therefore, each of these two processes can be described by a distribution function of relaxation times,  $g_\alpha(\log \tau)$  or  $g_\beta(\log \tau)$ , which shape can be temperature dependent, with an average (or characteristic) relaxation time  $\tau_\alpha(T)$  or  $\tau_\beta(T)$ . Below the glass transition temperature,  $T_g$ , where the  $\beta$  process can be observed detached from the  $\alpha$  process, the dielectric results of many polymers<sup>22</sup> indicate an Arrhenius temperature dependence, i.e.

$$\tau_\beta(T) = \tau_{\beta 0} \exp\left(\frac{E_0}{k_B T}\right) \quad (5)$$

where  $E_0$  represents an average activation energy of the

$\beta$  process,  $\tau_{\beta 0}$  is a preexponential factor and  $k_B$  is Boltzmann's constant. Taking into account eq 5,  $g_\beta(\log \tau)$  can be interpreted in terms of a distribution of activation energies.<sup>23</sup> A Gaussian distribution

$$g(E) = \frac{1}{\sigma_E \sqrt{2\pi}} \exp \left[ -\frac{1}{2} \left( \frac{E - E_0}{\sigma_E} \right)^2 \right] \quad (6)$$

of variance  $\sigma_E^2$  usually gives a good description of the experimental data at  $T < T_g$ , being  $\sigma_E$  approximately constant. The corresponding  $g_\beta(\log \tau)$  function is thus given by

$$g_\beta(\log \tau) = \frac{1}{\sigma \sqrt{2\pi}} \exp \left[ -\frac{1}{2} \left( \frac{\log \tau - \log \tau_\beta}{\sigma} \right)^2 \right] \quad (7)$$

with

$$\sigma = \frac{\log e}{k_B T} \sigma_E \quad (8)$$

The Arrhenius-like behavior of  $\tau_\beta(T)$  and the Gaussian-like shape of  $g_\beta(\log \tau)$  are known as the "characteristics of the dielectric  $\beta$  process". However, an unbiased application of the addition ansatz (eq 2 or 4) to fit dielectric relaxation data in the temperature range  $T > T_g$  (where the  $\alpha$  and  $\beta$  processes start to overlap) should admit that the temperature dependence of  $\tau_\beta$  and  $g_\beta(\log \tau)$  can change from the behavior observed below  $T_g$ . Taking this possibility into account, and in order to avoid any misunderstanding, we will call in the following  $\beta$  process to the secondary process at any temperature. It is worth emphasizing that this is only a renaming of the  $\beta$  process that tries to distinguish the secondary relaxation at any temperature from the extrapolation of the low-temperature behavior ( $\beta$  process). Thus, accordingly to this nomenclature, eqs 4 and 2 read respectively as

$$(\epsilon^*(\omega) - \epsilon_\infty)/(\epsilon_s - \epsilon_\infty) = \Phi^*(\omega) = f_\alpha \Phi_\alpha^*(\omega) + (1 - f_\alpha) \Phi_\beta^*(\omega) \quad (9)$$

$$\varphi(t) = f_\alpha \varphi_\alpha(t) + (1 - f_\alpha) \varphi_\beta(t) \quad (10)$$

When this approach is used for analyzing dielectric relaxation data of glass-forming polymers in the merging region of the segmental and secondary relaxations, the following results are usually obtained.

(i) The temperature dependence of  $\tau_\alpha$  follows a non-Arrhenius behavior, which can be described by means of the well-known Vogel–Fulcher equation,<sup>24</sup> i.e.

$$\tau_\alpha = \tau_{\alpha 0} \exp[B/(T - T_0)] \quad (11)$$

where  $B$ ,  $T_0$  (the ideal glass transition) and the limiting relaxation  $\tau_{\alpha 0}$ , are fitting parameters. The shape of  $g_\alpha(\log \tau)$  does not change very much with temperature, being the corresponding relaxation function in the time domain well described by a Kohlrausch–Williams–Watts (KWW)<sup>25,26</sup> function, i.e.

$$\varphi(t) = \exp \left[ -\left( \frac{t}{\tau_K} \right)^{\beta_K} \right] \quad (12)$$

where  $\tau_K$  would be the characteristic time of the  $\alpha$  relaxation and  $\beta_K$  accounts for the nonexponentiality of the relaxation, typically  $\beta_K \approx 0.4$ – $0.5$  and weakly

dependent on temperature. Moreover, the relative contribution of the  $\alpha$  process,  $f_\alpha$ , decreases as the temperature increases above  $T_g$ .

(ii)  $\tau_b(T)$  continuously deviates in the merging range from the extrapolation of the Arrhenius behavior observed at  $T < T_g[\tau_\beta(T)]$ .  $g_b(\log \tau)$  narrows with increasing temperature more than what should be expected from the extrapolation of the low temperature behavior, and simultaneously, it tends to become nonsymmetric. However, it is worthy of remark that, in the temperature range where these effects are observed, the parameters used to describe the shape of the  $\beta$  process are subjected to high uncertainties due the coupling with the ones describing the  $\alpha$  process. In connection with this, it is worth mentioning that in this framework at least seven parameters are commonly used to fit each single curve which is accessible only over about 4 decades.<sup>11,13,15,16</sup>

Now let us comment on the formalism of the WW ansatz as it has been applied to analyze dielectric relaxation data of a few glass-forming systems.<sup>11–14</sup> As it is has already been mentioned, this approach is in fact a simplification of the general concept proposed by Williams and Watts because, so far, only the autocorrelation terms of the reorientation of dipoles are taken into account. The WW ansatz used by us is easier formulated in the time domain as shown by eq 1, which can be rewritten as

$$\varphi(t) = f_\alpha \varphi_\alpha(t) + (1 - f_\alpha) \varphi_\alpha(t) \varphi_\beta(t) \quad (13)$$

In the WW ansatz  $1 - f_\alpha$  is related with the relaxation achieved in a fixed environment, i.e., with  $\varphi_\alpha(t) = 1$ . Therefore, in the dielectric relaxation case  $1 - f_\alpha$  gives the fraction of the dipole moment relaxation that is achieved by the local motions. Moreover, in this approach both  $\varphi_\alpha(t)$  and  $\varphi_\beta(t)$  are constructed at any temperature by means of the extrapolation of the temperature behavior observed in the temperature range where both processes are well separated, i.e., where they do not overlap very much. In principle, this is only a particular case. The core of the WW ansatz is the term combining the main and secondary relaxations, which reflects the statistical independence of both processes. However, this does not imply "a priori" that the  $\alpha$  and  $\beta$  processes behave as pure extrapolations from the low temperature. This is the simplest approach we can imagine, and due to this reason, we should test if it is possible to describe the data, within the experimental uncertainties, in this simple framework. As it was mentioned in the Introduction, eq 13 is also obtained in the framework of free-energy-landscape model for the simple case where no correlation exist between the mechanisms responsible of the  $\alpha$  and  $\beta$  process. Nevertheless, the model results show that the behavior observed for the loss spectrum in the merging region in the general case is hardly distinguishable, taking into account the usual experimental uncertainties, from that obtained in the particular case of completely uncorrelated relaxation processes.<sup>21</sup> In this approach we follow the general procedure to obtain the normalized relaxation from  $\varphi(t)$  using the Laplace transformation, i.e.

$$\Phi^*(\omega) = L_{i\omega}[-d\varphi(t)/dt] \quad (14)$$

where  $L_{i\omega}$  is the Laplace operator. Taking into account eqs 13 and 14, one obtains



$$[\epsilon^*(\omega) - \epsilon_\infty]/(\epsilon_s - \epsilon_\infty) = f_\alpha \Phi_\alpha^*(\omega) + (1 - f_\alpha) \Phi_{\beta\text{eff}}^*(\omega) \quad (15)$$

where using the same terminology introduced in ref 12,  $\Phi_{\beta\text{eff}}^*(\omega)$  represents  $L_{i\omega}\{-d[\varphi_\alpha(t)\varphi_\beta(t)]/dt\}$ . The algorithm used by us to construct  $\Phi_{\beta\text{eff}}^*(\omega)$  is that reported in ref 12, which can be summarized as follows: Both  $\varphi_\alpha(t)$  and  $\varphi_\beta(t)$  can be expressed respectively as

$$\varphi_\alpha(t) = \int_{-\infty}^{\infty} g_\alpha(\log \tau) e^{-t/\tau} d(\log \tau) \quad (16)$$

$$\varphi_\beta(t) = \int_{-\infty}^{\infty} g_\beta(\log \tau) e^{-t/\tau} d(\log \tau) \quad (17)$$

and therefore the term  $\varphi_{\beta\text{eff}}(t) = \varphi_\alpha(t) \varphi_\beta(t)$  results in

$$\varphi_{\beta\text{eff}}(t) = \varphi_\alpha(t) \varphi_\beta(t) = \int_{-\infty}^{\infty} g_\alpha(\log \tau) \left[ \int_{-\infty}^{\infty} g_\beta(\log \tau') \times e^{-t(1/\tau + 1/\tau')} d(\log \tau') \right] d(\log \tau) \quad (18)$$

from which  $\Phi_{\beta\text{eff}}^*(\omega)$  can be written as

$$\Phi_{\beta\text{eff}}^*(\omega) = \int_{-\infty}^{\infty} g_\alpha(\log \tau) \left[ \int_{-\infty}^{\infty} g_\beta(\log \tau') \times \frac{1}{1 + i\omega\left(\frac{1}{\tau} + \frac{1}{\tau'}\right)^{-1}} d(\log \tau') \right] d(\log \tau) \quad (19)$$

By comparing eqs 9 and 10 with eqs 13 and 15, we have to conclude that the addition ansatz and our simplified WW ansatz would be completely equivalent from a pure formal point of view if  $\Phi_b^*(\omega) \equiv \Phi_{\beta\text{eff}}^*(\omega)$  or if  $\varphi_b(t) \equiv \varphi_\alpha(t) \varphi_\beta(t)$  at any temperature. Below  $T_g$ , this equivalence results to be trivial; however, well above  $T_g$ , in the merging region  $\Phi_{\beta\text{eff}}^*(\omega)$  is directly determined from the low-temperature behavior whereas  $\Phi_b^*(\omega)$  is not. Therefore, the interesting range to experimentally compare the results obtained in the framework of the two different ansatzs is the range where the main and the secondary processes overlap (the merging region).

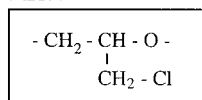
### III. Experimental Section

**Samples.** Poly(epichlorohydrin) (PECH), poly(vinyl methyl ether) (PVME), isopoly(methyl methacrylate) (i-PMMA), and poly(vinyl acetate) (PVAc) were obtained from Aldrich. Tetramethyl bisphenol polycarbonate (TMBPC) and poly(2-hydroxypropyl ether Bisphenol A), known as phenoxy (PH), were supplied by Bayer and Union Carbide, respectively. The chemical structure of the monomeric units is given in Figure 1. The glass transition temperatures of the samples, depicted in Table 1, were obtained from the middle point of the differential scanning calorimetry (DSC) trace measured at a heating rate of 10 K/min.

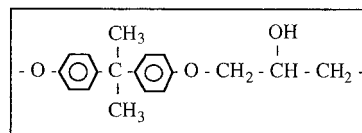
For the dielectric experiments, the samples were prepared on the electrode surface by solvent casting, with tetrahydrofuran (THF) as solvent. Special care was taken to ensure that no rest of the solvent remains in the sample.

**Dielectric Measurements.** Dielectric measurements were performed in the frequency domain from  $10^{-2}$ – $10^9$  Hz with a Novocontrol System by means of two different equipments. A Solartron-Schlumberger gain/phase analyzer SI1260 supplemented with a broad dielectric converter allowed the dielectric relaxation to be measured on the range  $10^{-2}$  up to  $10^7$  Hz. For higher frequencies ( $10^6$ – $10^9$  Hz), a Hewlett-Packard impedance analyzer HP4191A based on the principle of a reflectometer was used. The error in the determination of the loss tangent of the dielectric constant was around  $10^{-4}$  for the first set up and  $10^{-2}$  for the second one. Overlapping of the spectra at the same temperature was possible by means of the common decade of both equipments ( $10^6$ – $10^7$  Hz), and small corrections

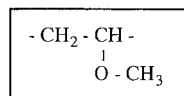
PECH



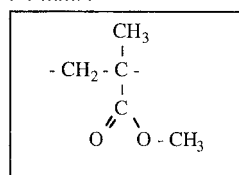
PH



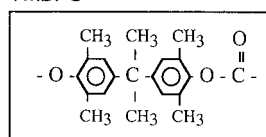
PVME



i-PMMA



TMBPC



PVAc

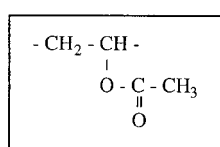


Figure 1. Chemical structure of the polymers investigated.

Table 1. Glass Transition Temperatures, Molecular Weights, and the Parameters Describing the Temperature Dependence of the  $\beta$  Relaxation for the Studied Polymers Where Parameter  $A$  Gives the Temperature Coefficient of  $\sigma_E(T)$ ,  $A = d\sigma_E/dT$

sample	$T_g$ (K)	$M_w$	$\sigma_E(T_g)$ (eV)	$A$ (eV/K)	$\tau_{\beta 0}$ (s)	$E_0$ (eV)
PECH	248	700 000	0.069	$-1.2 \times 10^{-4}$	$9.9 \times 10^{-13}$	0.25
PH	370	35 540	0.073	$-9.6 \times 10^{-5}$	$3.6 \times 10^{-16}$	0.45
PVME	247	21 900	0.044	$-4.4 \times 10^{-6}$	$2.6 \times 10^{-13}$	0.22
i-PMMA	322	300 000	0.12	$-4.2 \times 10^{-4}$	$1.6 \times 10^{-16}$	0.76
TMBPC	470		0.10	$-1.2 \times 10^{-4}$	$6.0 \times 10^{-16}$	0.85
PVAc	315	93 080	0.073	$-9.0 \times 10^{-5}$	$2.4 \times 10^{-12}$	0.32

were motivated by the uncertainties in the determination of the sample thickness. Measurements were made under isothermal conditions with temperature stability better than 0.1 K in all cases.

Sample holders, that act as electrodes, were parallel-plate capacitors of 20 mm diameter for the low frequency setup and 5 mm diameter for the high-frequency one. The distances between the electrodes were kept constant by insertion of Teflon (PTFE) spacers (0.1 mm thick) in the first case and quartz glass-fibers (0.05 mm thick) in the second one.

### IV. Results and Data Analysis

Figures 2–4 depict some representative data of the imaginary part of the dielectric constant for the studied polymers in three different temperature ranges. At

temperatures below  $T_g$ , the secondary relaxation is the main responsible of the dielectric loss features. This process is found in all the polymers investigated (see Figure 2). The low strength of the dielectric relaxation in this range makes difficult to have accurate measurements in the high-frequency range (above  $10^6$  Hz). In this range, the signal is of the same order of magnitude or lower than the accuracy provided by the experimental set up for all the systems. Therefore, below  $T_g$ , the reliable frequency range was  $10^{-2}$ – $10^6$  Hz.

As the temperature is increased, the  $\alpha$  relaxation starts to be observed in the frequency window (see Figure 3). The contributions to the dielectric losses corresponding to the segmental and secondary processes are distinctly. Except for PH, where the dielectric strength of the secondary relaxation is higher than that of  $\alpha$  relaxation, it can be seen that the dielectric dispersion is dominated by the  $\alpha$  process. For PH, TMBPC, and PVAc a conductivity contribution was also found at these temperatures in the low frequency side. This contribution has been successfully described by a  $\epsilon''(\omega) \propto 1/\omega$  law (dashed lines in Figure 3). This contribution was subtracted from the measured losses to obtain the dipolar contribution to  $\epsilon''(\omega)$ . In this temperature range, the secondary relaxation mainly contributes in the high-frequency range, and hence, high-frequency measurements are essential to have a good characterization of the process. The high-frequency values of  $\epsilon''(\omega)$  in this temperature range were found to be above the resolution limit of the high frequency setup. The reason for this is that the contribution of the secondary relaxation to the losses increases with temperature and, simultaneously, the  $\alpha$  relaxation starts to significantly contribute in this range.

At temperatures well above  $T_g$ , the shift of the  $\alpha$  peak to higher frequencies, which is much faster than that of the secondary relaxation, causes both peaks to become closer to each other. This can be seen in Figure 4 where a single peak shows up for PECH, i-PMMA, and TMBPC. On the contrary, for PH the separation between the  $\alpha$  and  $\beta$  processes still persists and the merging of both relaxations is not apparent. PVME and PVAc represent an intermediate situation.

As above commented upon, in this work we will compare the results obtained when the experimental data are fitted using the two previously described methods to analyze the merging region. It has already been shown above that for each method the dielectric relaxation process can be expressed in terms of the two distribution functions  $g_\alpha(\log \tau)$  and  $g_\beta(\log \tau)$  that contain the dynamical information on the  $\alpha$  process and the secondary relaxation. We have also mentioned that  $g_\beta(\log \tau)$  can usually be well described by means of a Gaussian-like function (eq 7). With respect to  $g_\alpha(\log \tau)$ , we have also commented that it usually corresponds to a relaxation process that is well described by the KWW function (eq 12) in the time domain. In the present study the following distribution function, proposed by Rajagopal et al.<sup>27</sup> has been used for  $g_\alpha(\log \tau)$

$$g(\log \tau) = \ln 10 \sqrt{2\beta} \left( \beta \frac{\tau}{\tau_c} \right)^{\beta/2(1-\beta)} \times \exp \left[ - (1 - \beta) \left( \beta \frac{\tau}{\tau_c} \right)^{\beta/2(1-\beta)} \right] \quad (20)$$

where  $\beta$  is a parameter related to the shape of the relaxation and  $\tau_c$  is a characteristic relaxation time of

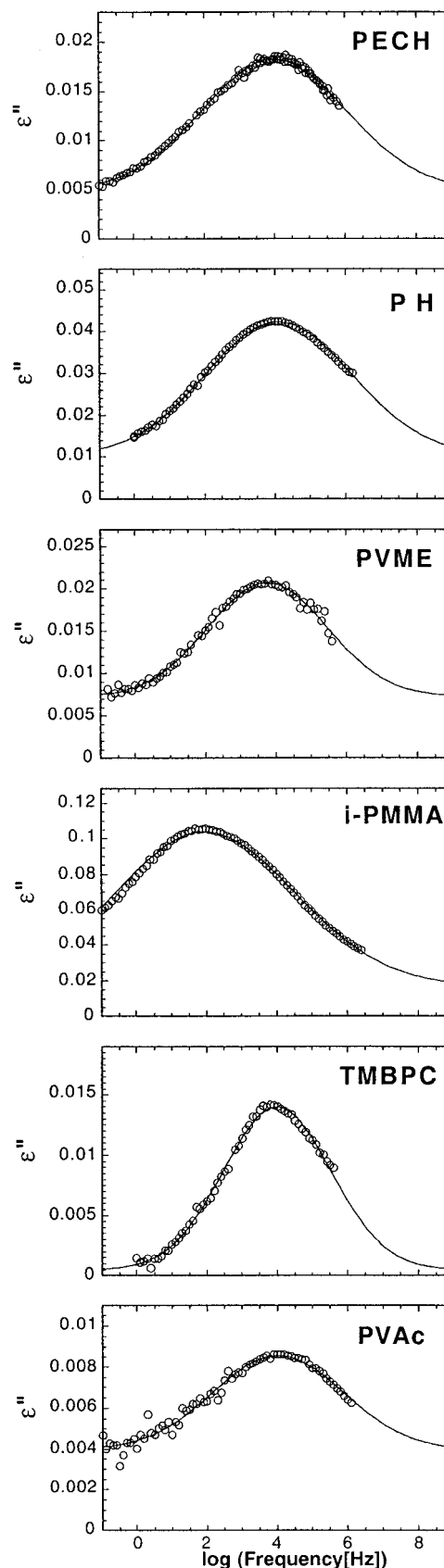


**Figure 2.**  $\beta$  relaxation isothermal loss curves for PECH, PH, PVME, i-PMMA, TMBPC, and PVAc at 178, 215, 138, 300, 410, and 240 K, respectively. Solid lines represent the obtained fittings as explained in the text.

the process. Equation 20 yields exactly a KWW function only for  $\beta = 0.5$ . Nevertheless, it has recently been shown<sup>28</sup> that, in the range  $0.2 < \beta < 1$ , eq 20 also

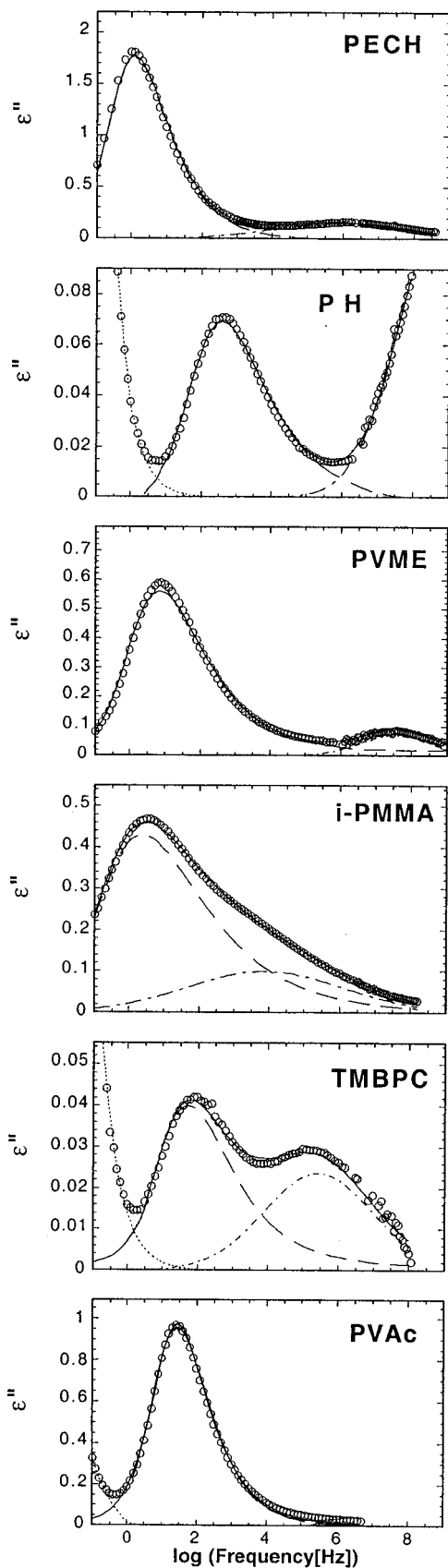


**Figure 3.** Isothermal loss curves slightly above  $T_g$  for PECH, PH, PVME, i-PMMA, TMBPC, and PVAc at 253, 385, 258, 335, 480, and 330 K, respectively. Solid lines represent the obtained fittings as explained in the text. Dashed lines show the contribution from the  $\alpha$  process, and dashed-dotted lines are the corresponding contribution from the  $b$  process. Dotted lines in PH, TMBPC, and PVAc represent the subtracted conductivity contribution.

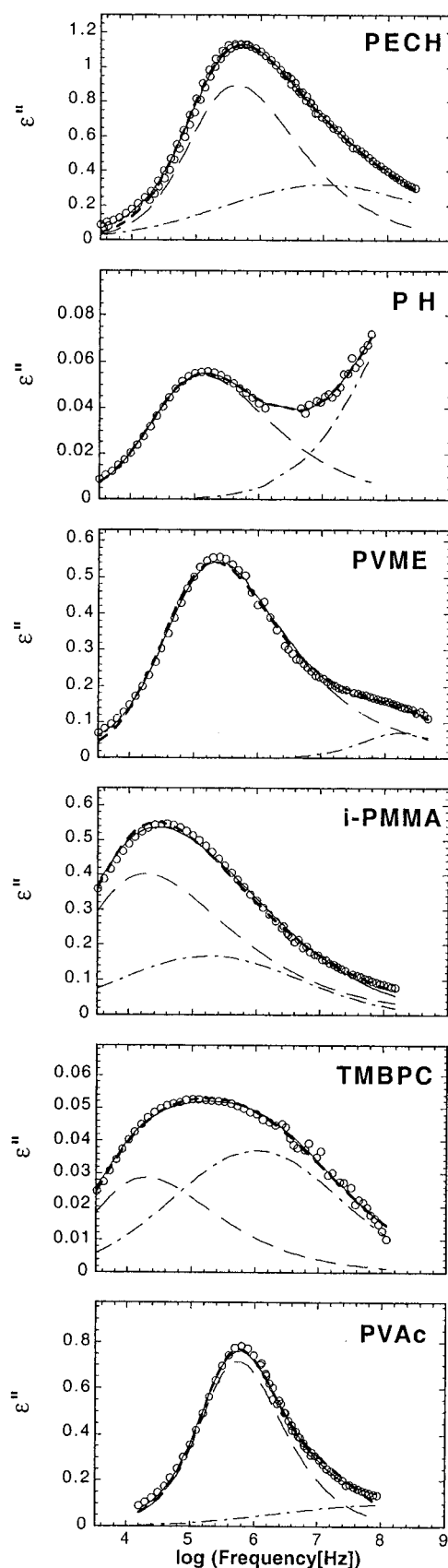


**Figure 4.** Isothermal loss curves well above  $T_g$  for PECH, PH, PVME, i-PMMA, TMBPC, and PVAc at 303, 405, 298, 370, 500, and 350 K, respectively. Solid lines represent the obtained fittings as explained in the text. Dashed lines show the contribution from the  $\alpha$  process, and dashed-dotted lines are the corresponding contribution from the  $b$  process. Thick dashed line shows the obtained fitting according to the WW ansatz.

provides a very good approximation to the KWW function. The KWW parameters and those of eq 20 are related in the following way:

$$\beta_K = 0.5 + 1.3237(\beta - 0.5) + 0.4648(\beta - 0.5)^2 + 1.2436(\beta - 0.5)^3 - 2.0129(\beta - 0.5)^4 \quad (21a)$$

$$\frac{\tau_K}{\tau_c} = 1 + 1.4459(\beta - 0.5) - 3.2598(\beta - 0.5)^2 + 2.385(\beta - 0.5)^3 - 2.1424(\beta - 0.5)^4 \quad (21b)$$

Hence, for a wide range of values of  $\beta$ , using eq 20 is equivalent to assuming a KWW function for  $\varphi(t)$ . Starting from the distribution functions given by eqs 7 and 20, the dielectric relaxation functions have been evaluated in the two different approaches by using eqs 9 and 15. The model parameters were extracted at each temperature by fitting the experimental losses using standard minimization procedures. Note that in both ansatz there are, in principle, the same six fitting parameters, namely:  $\Delta\epsilon$  and  $f_a$ , accounting respectively for the total and relative dielectric relaxation strength,  $\tau_K$  and  $\beta_K$ , characterizing the dynamics of the  $\alpha$  process, and  $\tau_b$  and  $\sigma$ , characterizing the dynamics of the  $\beta$  process. Four different temperature ranges were considered on fitting.

(i) As it was commented above, well below  $T_g$ , the secondary relaxation is the main contribution to the dielectric losses in the measuring window, since the characteristic time of the  $\alpha$  relaxation is extremely large. Therefore, one would expect that the dielectric losses corresponding to the first term in eqs 9 and 15 would be negligible. However, in the experimental spectra of all the samples, the loss peak assigned to secondary relaxation is superimposed on a nearly flat contribution. The origin of such contribution, which increases when approaching  $T_g$ , is not clear although it might be due to the so-called high-frequency wing of the  $\alpha$  relaxation.<sup>29</sup> Such a wing, showing a weak frequency dependence, has been reported at temperatures well below  $T_g$  in those systems which do not present a clear secondary relaxation.<sup>29</sup> Thus, in the fitting procedure well below  $T_g$ , the contribution to the dielectric losses of the  $\alpha$  process was approximated by a flat background.

(ii) At temperatures close but still below  $T_g$ , the contribution of the  $\alpha$  process starts to be more apparent since in this temperature range the  $\alpha$  process is close to the slower limit of the experimental window. The contribution of the  $\alpha$  relaxation in this range decreases with frequency following a power law. This contribution would correspond to the segmental dynamics, which below  $T_g$  exists in an out-of-equilibrium state with a time scale faster than that expected for the equilibrated polymer melt.<sup>30</sup> This fact makes the power law contribution to be apparent from temperatures well below  $T_g$ , typically  $T_g - 40$  K.

(iii) At temperatures from  $T_g$  up to around  $T_g + 40$  K, the  $\alpha$ -relaxation peak appears rather well separated from the contribution of the secondary processes. In this range a fitting in the framework of the addition ansatz was performed allowing all the parameters in eq 9 to be free. However, as aforementioned, in the WW ansatz the parameters characterizing the secondary relaxation, namely  $\sigma$  and  $\tau_b$ , were fixed in eq 15 to the values extrapolated from the low-temperature behavior (regions i and ii). This difference between the two

methods of analysis above  $T_g$  is related to the above-mentioned fact that, whereas below  $T_g$  both methods are equivalent, above  $T_g$  the secondary relaxation is determined from that observed below  $T_g$  in the WW ansatz, while in the addition ansatz it might be different.

(iv) At even higher temperatures, the two processes are getting closer in frequency for most of the polymers (merging region), whereas for others the secondary relaxation is nearly out of the frequency window experimentally covered. In both cases, a strong coupling between the fitting parameters appears, mainly in the framework of the addition ansatz since there are more fitting parameters. Thus, unrealistic values of the parameters can yield reasonable fitting curves, and therefore, the extrapolation of some parameters was needed to obtain moderate uncertainties in the values determined in the fitting procedure (see below).

Following the procedure described above, first the experimental loss curves were fitted in regions i and ii. It is important to note that the main part of the  $\alpha$  process is out of the accessible frequency window in these regions and the two ansatzs, being equivalent, yield the same curve fitting and parameter values. The solid lines in Figure 2 show some representative curve fittings in region i. We found that, below  $T_g$ , the average relaxation time of the secondary relaxation follows a well-defined Arrhenius behavior (eq 5) for all the polymers (see Figure 5). The values of the corresponding Arrhenius parameters obtained are listed in Table 1. The activation energy seems to be somehow correlated with the glass transition temperature according with that found in recent studies.<sup>7,14,31</sup> On the other hand,  $\sigma$  decreases with temperature as expected from eq 8 with a nearly constant value of  $\sigma_E$ . The weak temperature dependence of  $\sigma_E$  can be accounted by a linear fit with the parameters given in Table 1. From that fit it is found that the ratio  $\sigma_E(T_g)/E_0$  is around 20% for all the polymers investigated.

In region iii, the main part of the  $\alpha$  process is inside the frequency window; thus, it can be completely characterized in this region. Note that in region iii, the two methods of analysis are not strictly equivalent since in the WW ansatz framework the parameters  $\tau_b$  and  $\sigma_E$  are taken from the behavior determined previously in regions i and ii whereas in the addition ansatz  $\tau_b$  and  $\sigma$  remain free. This ensures that, in the WW ansatz framework, the number of fitting parameters is reduced from 6 to 4. Despite that, the fitting curves resulting from both procedures are hardly distinguishable. Some representative fitting curves are depicted in Figure 4. The parameters  $\tau_b$  and  $\sigma_E$  obtained in this region in the addition ansatz framework remain close to the ones extrapolated from low temperature (values used in the WW analysis). Concerning the other parameters, we found that, by using both methods of analysis, the shape of the  $\alpha$  process remains nearly temperature independent for PECH and narrows moderately with  $T$  for PH, PVME, and TMBPC. On the contrary, for PVAc and i-PMMA, the narrowing is more pronounced near  $T_g$ . However, for all the polymers the shape parameter becomes nearly temperature independent at high temperatures. To account for these behaviors we have described the temperature dependence of the shape parameter  $\beta_K$  in all the polymers investigated using the following function  $\beta_K(T) = 1 - \exp[-c_1(T - c_2)]$ , which has been proposed elsewhere.<sup>10,32</sup> The values of  $c_1$  and  $c_2$ , as well as the values of  $\beta_K$  at  $T_g$ , corresponding to



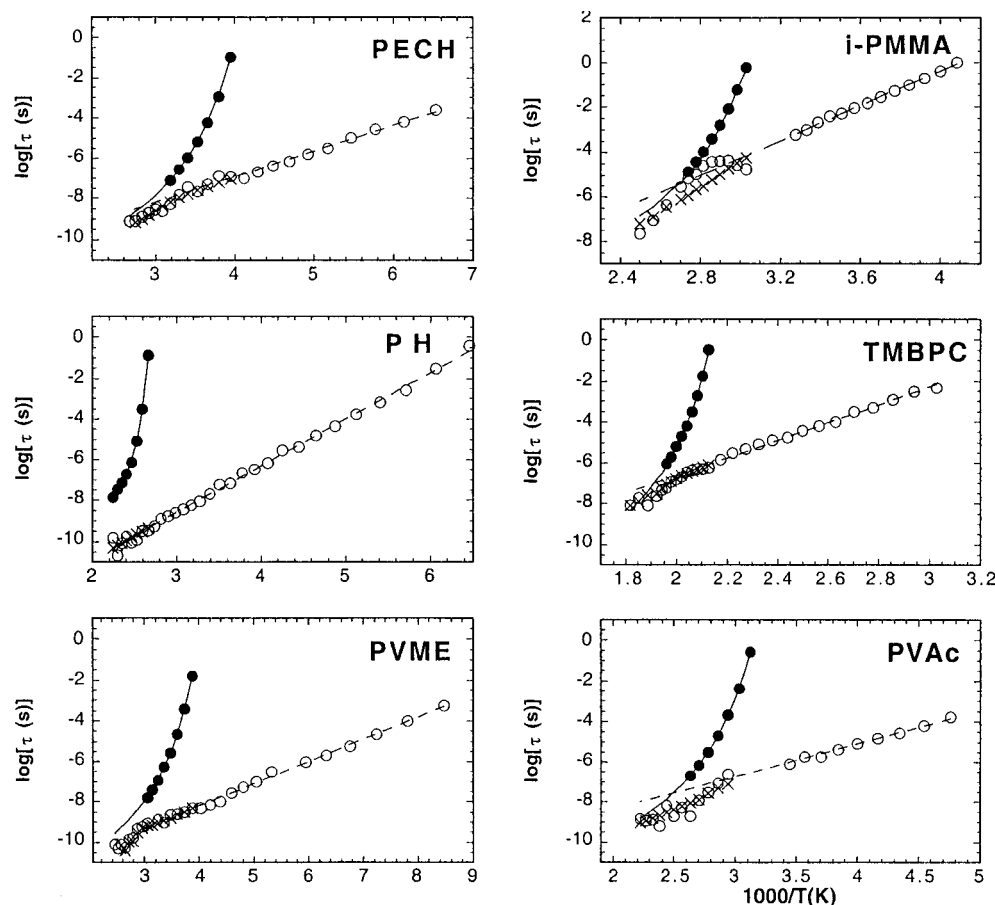


**Figure 5.** Relaxation times for the different studied processes: Full circles represent the obtained relaxation times for the  $\alpha$  process, and the solid line represents the extrapolated Vogel–Fulcher behavior (see Table 2 for parameters). Open circles show the relaxation times of  $\beta$  process and dashed line corresponds to low-temperature Arrhenius behavior (see Table 1 for parameters). Crosses show the characteristic times corresponding to  $\Phi^*_{\text{eff}}(\omega)$ .

**Table 2. Parameters Describing the Temperature Dependence of the  $\alpha$  Relaxation of the Studied Compounds Where the Parameters  $c_1$  and  $c_2$  Correspond to the Equation  $\beta_K(T) = 1 - \exp[-c_1(T - c_2)]$**

sample	$\beta_K(T_g)$	$c_1$ ( $K^{-1}$ )	$c_2$ (K)	$\tau_{\alpha 0}$ (s)	$B$ (K)	$T_0$ (K)
PECH	0.53	$3.5 \times 10^{-5}$	$-20556$	$7.5 \times 10^{-13}$	1281	202.9
PH	0.35	$6.3 \times 10^{-3}$	302	$4.2 \times 10^{-11}$	553	349.5
PVME	0.35	$5.1 \times 10^{-3}$	167	$2.7 \times 10^{-13}$	1392	201.6
i-PMMA	0.22	$5.2 \times 10^{-3}$	273	$9.5 \times 10^{-12}$	1167	282.1
TMBPC	0.39	$5.2 \times 10^{-3}$	377	$3.6 \times 10^{-14}$	1589	415.6
PVAc	0.48	$6.75 \times 10^{-3}$	218	$5.2 \times 10^{-13}$	1525	263.4

the different polymers are listed in Table 2. On the other hand, the values obtained for the relaxation time of the  $\alpha$  process are also observed to be very similar in both cases, although small differences become apparent when the merging region is approached. Nevertheless, these differences are so small that they cannot be detected in Figure 5. Equation 11, with the parameters listed in Table 2, gives a good description of the two sets of  $\tau_\alpha$  data in this region. With respect to  $\Delta\epsilon$  and  $f_\alpha$ , we found that  $\Delta\epsilon$  is hardly sensitive to the analysis procedure, but the values of  $f_\alpha$  start to differ significantly when the merging region is approached (see Figure 6).

As commented above, the temperature behavior of the dynamic parameters in region iv cannot be determined with sufficient accuracy by allowing all the fitting parameters to be free in both of the methods. Thus, in this region we have fixed some fitting parameters, mainly for the addition ansatz but also in the framework of the WW ansatz. In the former case we have extrapolated  $\beta(T)$  and  $\tau_\alpha(T)$ , i.e., the dynamic parameters

characterizing the  $\alpha$  process, according to the temperature dependencies found in region iii. This choice will evidence any possible change in the temperature dependence of the parameters describing the  $\beta$  process in the merging region. However, in the Williams approach, where  $\sigma(T)$  and  $\tau_\beta(T)$  are already extrapolated from the low temperature, only  $\beta(T)$  was fixed in region iv. In this way, the number of free fitting parameters in this region becomes four for the addition ansatz and three for the WW ansatz. From the fitting obtained by means of the two approaches, it follows that both the curve fitting and the fitting parameters are different in this region for those polymers where the main and the secondary processes are getting very close (merging process). In both analyses, the fitting curves obtained in region iv are in rather good agreement with experimental data, even for the polymers where the overlapping of the  $\alpha$  and  $\beta$  relaxations is strong. However, the addition ansatz does not produce a better fitting of the experimental data than the one obtained using the WW ansatz (see Figure 7), although an additional fitting parameter is used in the former case. It is noteworthy that, in the procedure followed here, the shape of  $g_b(\log \tau)$  is assumed to remain symmetric in this region. However, what is found when the addition ansatz is used without any restriction for the shape of  $g_b(\log \tau)$  is that it tends to become asymmetric in the merging range. This will be discussed in more detail in the next section. In summary, it is apparent that, for those polymers where the merging process is accessible, the



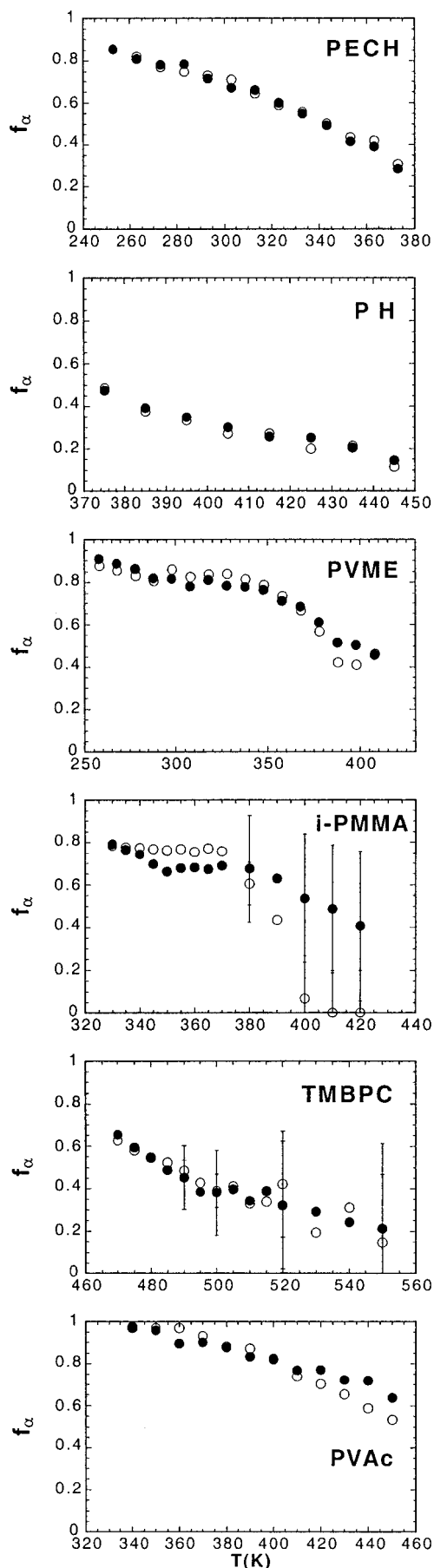


**Figure 6.** Obtained relative relaxation strengths,  $f_\alpha$ , for all the studied polymers. Full symbols correspond to the addition ansatz and open symbols to the WW one.

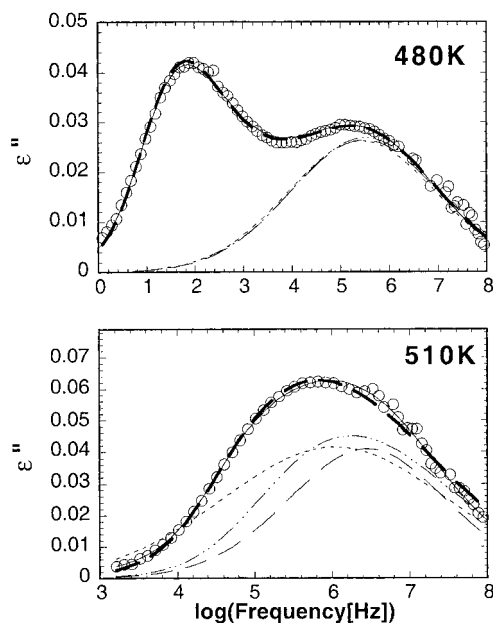


**Figure 7.** Dielectric loss curves for TMBPC at 480 and 510 K. Lines are fittings according to the addition ansatz (solid) and to the WW one (thick dashed). Dashed line represents the b process from the addition ansatz, dashed-dotted line the  $\beta$ -effective process from the WW ansatz and the dotted line the extrapolated  $\beta$  relaxation that would correspond to parameters listed in Table 1.

parameters obtained using the two approaches are different in this region. On the contrary, for the polymers where the secondary relaxation and the  $\alpha$  process remain far from each other, both methods yield equivalent results also in region iv.

## V. Discussion

The results shown above demonstrate that the experimental data in the merging region of different polymers can be well described using the two different methods of analysis. In both cases,  $f_\alpha$  tends to decrease with increasing temperature above  $T_g$  (see Figure 6) and would eventually vanish at high temperatures, although the uncertainty in the value of  $f_\alpha$  in this range becomes extremely large, independently of the method used. The rather similar values of  $f_\alpha$  found using the two ways of analysis imply that the relaxation functions  $\Phi_b^*(\omega)$  and  $\Phi_{\beta\text{eff}}^*(\omega)$  should be hardly distinguishable. To compare the behavior of  $\Phi_b^*(\omega)$  and  $\Phi_{\beta\text{eff}}^*(\omega)$  in detail, in Figure 5 we have depicted the characteristic times obtained from the maximum of the losses associated with  $\Phi_{\beta\text{eff}}^*(\omega)$  in comparison with the values of the characteristic times of the  $\beta$  process determined using the addition ansatz. When the main and the secondary relaxations are well separated both coincide, as expected, with the line describing  $\tau_\beta(T)$ , i.e., the low temperature behavior of the characteristic time of the secondary relaxation. Moreover, approaching the merging region (but in some cases a few tens of degrees below), both sets of data deviate similarly from the extrapolation of the low-temperature  $\tau_\beta(T)$ . Therefore, one of the most relevant features of the comparison is that for all the polymers  $\tau_b(T)$  is found to be nearly equivalent to  $\tau_{\beta\text{eff}}(T)$ . To further test the similarities between  $\Phi_b^*(\omega)$  and  $\Phi_{\beta\text{eff}}^*(\omega)$ , in Figure 7 we show, as an example, the loss spectrum of TMBPC at two temperatures, one close to  $T_g$  and the other in the merging region. As can be seen, the secondary relax-

ation near  $T_g$  is much faster than the  $\alpha$  one and therefore the relaxation times  $\tau_{\beta\text{eff}}$  and  $\tau_b$  are just the same, as well as the contribution to the losses of  $\Phi_{\beta\text{eff}}''(\omega)$  and  $\Phi_b''(\omega)$ . Similar results are obtained for the rest of the polymers. Thus, as shown above, no differences exist between both methods of analysis at temperatures close to  $T_g$ . At higher temperatures, the situation changes gradually, and the description of the two approaches is no longer exactly equivalent in the merging range. As can be seen in Figure 7b, whereas  $\Phi_b''(\omega)$  remains (by assumption) symmetric in the log  $\omega$  scale,  $\Phi_{\beta\text{eff}}''(\omega)$  is markedly asymmetric. Nevertheless, the frequencies at the maxima of  $\Phi_{\beta\text{eff}}''(\omega)$  and  $\Phi_b''(\omega)$  are close and, furthermore, their widths remain similar and clearly smaller than that expected from the extrapolation of the secondary relaxation spectrum from low temperatures. The similarity found between  $\Phi_{\beta\text{eff}}^*(\omega)$  and  $\Phi_b^*(\omega)$  is not trivial (note that  $\Phi_{\beta\text{eff}}^*(\omega)$  is constructed from the extrapolation of the low temperature relaxation behavior) and in fact implies that the results obtained in using the addition ansatz give support and justify the validity of the WW ansatz. It is worthy of remark that this result directly emerges from experiments performed on very different systems and not from any particular interpretation of the data.

From the above discussion, the main difference between the two methods of analysis used in the merging region is the different interpretation of the polymer dynamics far above  $T_g$ . In the WW ansatz, the high temperature dynamics is directly connected with the dynamical behavior observed at low temperature. However, in the addition ansatz the dynamics at temperatures around and above the merging region have to be interpreted as produced by a physical mechanism different from those responsible of the  $\alpha$  and  $\beta$  relaxations observed at low temperatures. Moreover, whereas in the addition ansatz the experimental finding that  $f_\alpha$  seems to extrapolate to zero at high temperature is interpreted as a vanishing of the  $\alpha$ -relaxation process (and therefore of the cooperativity), in the WW ansatz this interpretation does not hold. The reason is that in the WW ansatz  $\Phi_{\beta\text{eff}}^*(\omega)$  represents the convolution term of  $\Phi_\alpha^*(\omega)$  and  $\Phi_\beta^*(\omega)$ , being its behavior dominated by the fastest of the two processes. Since at very high temperatures the characteristic time of the  $\beta$  process would become longer than that of the  $\alpha$  relaxation, in this range  $\Phi_{\beta\text{eff}}^*(\omega) \cong \Phi_\alpha^*(\omega)$ , which yields  $\Phi^*(\omega) \cong \Phi_\alpha^*(\omega)$  for any value of  $f_\alpha$ . Therefore, in the framework of the WW ansatz the very high-temperature dynamics is governed, mainly, by the mechanism responsible of the  $\alpha$  relaxation. Thus, within the WW ansatz,  $f_\alpha$  cannot be interpreted, in the high-temperature range, as the relative contribution of the  $\alpha$  process to the whole relaxation. As abovementioned, in the WW picture  $f_\alpha$  indicates the part of the time decay that would not occur if the molecular environment does not change.

As was already commented upon in the Introduction, the WW ansatz arises naturally on the basis of a free-energy landscape model for the dynamics of glass-forming systems when a slow secondary relaxation is considered.<sup>21</sup> In this model the secondary relaxation is modeled by a superposition of simple two-site angular jumps within a cone of angle  $\theta$ , which, within the assumptions of the model, determines the temperature behavior of  $f_\alpha$ .<sup>21</sup> To compare the  $f_\alpha(T)$  behavior obtained for the different polymers, in Figure 8 we have depicted the  $f_\alpha$  values obtained using the WW ansatz as a

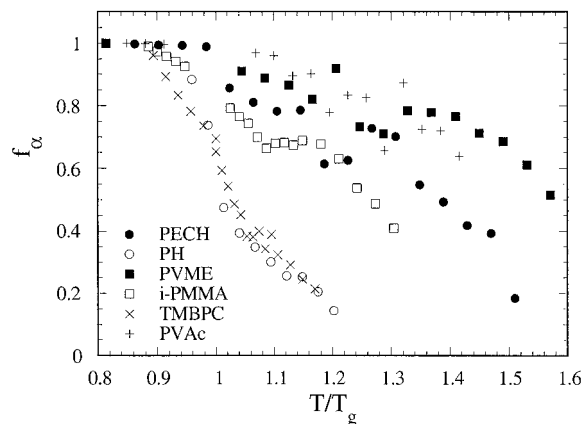


**Figure 8.** Temperature dependence of  $f_\alpha$  (WW ansatz) scaled according to the  $T_g$  values corresponding to the different polymers.

function of  $T/T_g$ . The values of  $f_\alpha$  appearing in the figure for  $T < T_g$  have been calculated as  $f_\alpha = \Delta\epsilon_\alpha / [\Delta\epsilon_\beta + \Delta\epsilon_\alpha(T)]$ ,  $\Delta\epsilon_\alpha(T)$  being the extrapolation of the  $\Delta\epsilon_\alpha$  experimental behavior according with a Curie–Weiss law. In the representation used in Figure 8 a direct comparison among the different polymers and also with the predictions of the landscape model is straightforward. From this comparison, it turns out that  $f_\alpha(T/T_g)$  strongly depends on the type of polymer considered. Our results indicate that, for TMBPC and PH, both having phenyl rings in the main chain,  $f_\alpha(T/T_g)$  shows a very rapid decrease above  $T_g$  whereas for the vinyl polymers investigated, PVME and PVAc, the decrease of  $f_\alpha(T/T_g)$  is moderate. For the other two polymers, we found intermediate situations. By comparison of the results shown in Figure 8 with those obtained from the free-energy landscape model (Figure 2b in ref 21), some estimates of the  $\theta$  values corresponding to the polymers investigated can be found. The values of  $\theta$  so obtained are in the ranges: 70–80° for TMBPC and PH, 10–20° for PVAc and PVME, and 30–40° for PECH, and  $\theta \cong 45$ –55° for i-PMMA. For the results of 1,4-polybutadiene reported previously,<sup>12</sup> the estimated value was 60–70°, which is not very different from the values determined by us for TMBPC and PH. Thus, it seems that  $f_\alpha(T/T_g)$ , and therefore the value of  $\theta$ , is related to the monomeric structure of the polymer.

## VI. Conclusions

We have shown that the relaxation behavior of a series of polymers in the high temperature range, where the main and the secondary relaxations merge, can successfully be described using two different approaches. Although these approaches have similarities from a formal point of view, they imply very different interpretations of the polymer dynamics at temperatures well above  $T_g$ . When the results obtained from the two analysis methods are compared, it is found that the results obtained with the addition method support the validity of the WW ansatz. In particular, it is found that the apparent deviation of  $\tau_b(T)$  from the Arrhenius behavior deduced from low temperature can be interpreted as a consequence of the convolution term of the  $\alpha$  and  $\beta$  processes ( $\Phi_{\beta\text{eff}}$ ). Since in the high-temperature limit  $\Phi_{\beta\text{eff}}$  becomes similar to  $\Phi_\alpha$ , the polymer dynamics in this range will mainly be determined by the mechanisms responsible of the  $\alpha$  relaxation independently of the value of  $f_\alpha$ . This point of view is opposite to the

interpretation of the finding that the parameter  $f_\alpha$  tends to become zero at high temperatures as a proof of the vanishing of the cooperativity in the polymer dynamics. In summary, the WW approach provides a natural explanation for the observed temperature dependence of the dielectric response in the merging regime on the basis of the low-temperature behavior. This finding, which applies not only to the six polymers investigated here but also to other polymeric and nonpolymeric systems,<sup>11–15</sup> strongly supports the molecular grounds for the merging scenario from which the WW ansatz is derived. In particular, recent calculations based on a free-energy landscape model for the dynamics of glass-forming systems, which also support the WW ansatz analysis, allow a connection of the observed relaxation behavior with the molecular mechanisms responsible of the dynamics. Namely, on the basis of the assumptions of this landscape model, the temperature dependence of  $f_\alpha$  is determined by the angle  $\theta$  of the cone on which the restricted angular fluctuations associated with the  $\beta$  relaxation occur. Following this procedure, it turns out that the values of  $\theta$  obtained are somehow correlated with the chemical structure of the polymers investigated, with  $\theta$  being large for the polymers with phenyl rings in the backbone and smaller for the vinyl polymers.

**Acknowledgment.** This work has been supported by the Spanish Ministry of Education (MEC) (Project PB97-0638), the Government of the Basque Country (Project GV-PI/1998/20), and the University of the Basque Country (Projects 206.215-G20/98). The authors thank Gipuzkoako Foru Aldundia, and Iberdrola S.A. for partial financial support. D.G. is thankful for a grant of the Spanish Ministry of Education. Support from "Donostia International Physics Center" is also acknowledged.

## References and Notes

- (1) Anderson, P. W. *Science* **1995**, *267*, 1615.
- (2) McCrum, N. G.; Read, B. E.; Williams, G. *Anelastic and Dielectric Effects in Polymeric Solids*; London: Wiley, 1967 (reprint: Dover: New York, 1991).
- (3) *Basic Features of the Glassy State*; Colmenero, J., Alegria, A., Eds.; World Scientific: Singapore, 1990.
- (4) Götze, W. In *Liquids, Freezing and the Glass Transition*; Hansen, J. P., Levesque, D., Zinn-Justin, J., Eds.; North-Holland: Amsterdam, 1991.
- (5) Johari, G. P.; Goldstein, M. *J. Chem. Phys.* **1970**, *53*, 2372.
- (6) Johari, G. P.; Goldstein, M. *J. Phys. Chem.* **1970**, *74*, 2034; *J. Chem. Phys.* **1971**, *55*, 4245.
- (7) Kudlik, A.; Tschirwitz, C.; Benkhof, S.; Blochowicz, T.; Rössler, E. *Europhys. Lett.* **1997**, *40*, 649.
- (8) Wu, L. *Phys. Rev. B* **1991**, *43*, 9906.
- (9) Arbe, A.; Colmenero, J.; Frick, B.; Monkenbusch, M.; Richter, D. *Macromolecules* **1998**, *31*, 4926.
- (10) Alegria, A.; Colmenero, J.; Mari, P. O.; Campbell, I. A. *Phys. Rev. E* **1999**, *59*, 6888.
- (11) Williams, G.; Watts, C. D. In *NMR, Basic Principles and Progress*; Diehl, P., Fluck, E., Kosfeld R., Eds.; Springer-Verlag: Berlin, 1971; Vol. 4, p 271–285. Williams, G. *Adv. Polym. Sci.* **1979**, *33*, 60.
- (12) Arbe, A.; Richter, D.; Colmenero, J.; Farago, B. *Phys. Rev. E* **1996**, *54*, 3853.
- (13) Alvarez, F.; Hoffman, A.; Alegria, A.; Colmenero, J. *J. Chem. Phys.* **1996**, *105*, 432.
- (14) Bergman, R.; Alvarez, F.; Alegria, A.; Colmenero, J. *J. Chem. Phys.* **1998**, *109*, 7546.
- (15) Kudlik, A.; Tschirwitz, C.; Blochowicz, T.; Benkhof, S.; Rössler, E. *J. Non-Cryst. Solids* **1998**, *235–237*, 406.
- (16) Kahle, S.; Korus, J.; Hempel, R.; Unger, R.; Höring, S.; Schröter, K.; Donth, E. *Macromolecules* **1997**, *30*, 7214.
- (17) Schröter, K.; Unger, R.; Reissig, S.; Garwe, F.; Kahle, S.; Beiner, M.; Donth, E. *Macromolecules* **1998**, *31*, 8966.
- (18) Casalini, R.; Fioretto, D.; Livi, A.; Lucchesi, M.; Rolla, P. A. *Phys. Rev. B* **1997**, *56*, 3016.
- (19) Capaccioli, S.; Corezzi, S.; Gallone, G.; Rolla, P. A.; Comez, L.; Fioretto, D. *J. Non-Cryst. Solids* **1998**, *235–237*, 576.
- (20) Diezemann, G. *J. Chem. Phys.* **1997**, *107*, 10112.
- (21) Diezemann, G.; Mohanty, U.; Oppenheim, I. *Phys. Rev. E* **1999**, *59*, 2067.
- (22) Arbe, A.; Gómez, D.; Colmenero, J.; Richter, D.; Farago, B. *Phys. Rev. E* **1999**, *60*, 1103.
- (23) Deegan, R. D.; Nagel, S. R. *Phys. Rev. B* **1995**, *52*, 5653. Birge, N. O.; Jeong, Y. H.; Nagel, S. R.; Bhattacharya, S.; Susman, S. *Phys. Rev. B* **1984**, *30*, 2306.
- (24) Vogel, H. *Physik. Z.* **1921**, *22*, 645. Fulcher, G. S. *J. Am. Ceram. Soc.* **1925**, *8*, 339.
- (25) Kohlrausch, F. *Pogg. Ann. Phys.* **1863**, *119*, 352.
- (26) Williams, G.; Watts, D. C. *Trans. Faraday Soc.* **1970**, *66*, 80. Williams, G. In *Materials Science & Technology Series. Vol. 12. Structure and properties of polymers*; Thomas, E. L., Ed.; VCH Publ.: Weinheim, Germany, 1993.
- (27) Rajagopal, A. K.; Ngai, K. L. In *Relaxation in Complex Systems*; Ngai, K. L., Wright, G. R., Eds.; North-Holland: Amsterdam, 1991.
- (28) Gómez, D.; Alegria, A. *J. Non-Crystalline Solids*, in press.
- (29) Leheny, R. L.; Nagel, S. R. *Europhys. Lett.* **1997**, *39*, 447.
- (30) Alegria, A.; Guerra-Echevarria, E.; Goitiandia, L.; Telleria, I.; Colmenero, J. *Macromolecules* **1995**, *28*, 1516. Alegria, A.; Goitiandia, L.; Telleria, I.; Colmenero, J. *Macromolecules* **1997**, *30*, 3881.
- (31) Frick, B.; Richter, D. *Science* **1995**, *267*, 1939.
- (32) Cutroni, M.; Mandanici, A.; Piccolo, A. *J. Phys.: Condens. Matter.* **1995**, *7*, 6781.

MA992039Y